

THE OBSERVATION OF POSSIBLE RECONNECTION EVENTS IN THE BOUNDARY CHANGES OF SOLAR CORONAL HOLES

S.W. Kahler

Physics Research Division, Emmanuel College, 400 The Fenway, Boston
MA 02115

J.D. Moses

American Science and Engineering, Inc., Ft. Washington,
Cambridge MA 02139

Abstract. Coronal holes are large scale regions of magnetically open fields which are easily observed in solar soft X-ray images. The boundaries of coronal holes are separatrices between large-scale regions of open and closed magnetic fields where one might expect to observe evidence of solar magnetic reconnection. Previous studies by Nolte and colleagues using Skylab X-ray images established that large scale ($\sim 9 \times 10^4$ km) changes in coronal hole boundaries were due to coronal processes, i.e., magnetic reconnection, rather than to photospheric motions. Those studies were limited to time scales of about one day, and no conclusion could be drawn about the size and time scales of the reconnection process at hole boundaries.

We have used sequences of appropriate Skylab X-ray images with a time resolution of about 90 min during times of the central meridian passages of the coronal hole labelled "Coronal Hole 1" to search for hole boundary changes which can yield the spatial and temporal scales of coronal magnetic reconnection. We find that 29 of 32 observed boundary changes could be associated with bright points. The appearance of the bright point may be the signature of reconnection between small-scale and large-scale magnetic fields. The observed boundary changes contributed to the quasi-rigid rotation of Coronal Hole 1.

Introduction

Coronal holes are regions of unusually low density and temperature in the solar corona. They are present at all phases of the solar cycle, but reach their maximum extent in the two or three years before solar minimum. Over a decade ago Krieger (1977) in his review of the temporal behavior of coronal holes posed several fundamental questions about the evolution of holes that have yet to be completely answered. In particular, he asked: 1) What is the relationship between the stochastic diffusion of photospheric magnetic flux and the large-scale boundary changes? 2) What is the characteristic time scale for coronal hole boundary changes? 3) What is the role of emerging flux? 4) Are the large-scale boundary shifts cases of field line reconnection or of the evacuation of previously opened field lines?

An examination of the boundary changes of coronal holes was carried out by Nolte and colleagues (Nolte et al., 1978 a,b,c) using Skylab X-ray images from the period of May to November 1973. For each central meridian passage (CMP) of the Skylab coronal holes they compared the boundaries observed in three X-ray images: an image at CMP, an image 1 day earlier, and an image 1 day later. This procedure allowed them to study boundary changes with a time resolution of 1 day. Because of a concern with the possibility that the boundaries could move as a result of the diffusive motion of the field lines, they considered two classes of changes. Small-scale changes ranged from $\approx 1.2 \times 10^4$ km, the smallest changes they could measure to 9×10^4 km. Large-scale changes were those exceeding 9×10^4 km, ≈ 3 times the average supergranulation cell length. This criterion was used to preclude the possibility that large-scale changes could arise from the chance association of random motions. Nolte et al. (1978a) found statistically that about 38% of the boundary lengths showed a significant change over 1 day. The small-scale changes accounted for 70% of this total, and the large-scale changes for the remaining 30%.

In their second paper Nolte et al. (1978b) inferred that the large-scale changes (which they referred to as "sudden") must involve a process different from that of at least some of the small-scale changes because the large-scale changes were found to account for most of the long-term (rotation-to-rotation) changes in coronal hole areas whereas the small-scale changes seemed poorly correlated with the long-term changes.

In the third paper Nolte et al. (1978c) studied the specific coronal structures which seemed to play roles in the growth and decay of coronal holes. They found a general agreement with the hypothesis that holes are born and grow in conjunction with active regions. They also found evidence that holes decayed when the number of X-ray bright points in the longitude bands containing the holes was relatively high. X-ray bright points are pointlike X-ray emitting features associated with small bipolar magnetic features (Golub et al., 1974).

We might expect that the detailed studies of Nolte et al. (1978 a,b,c) would have explored Krieger's (1977) questions to the limit of the X-ray observations. However, those studies were based only on comparisons of X-ray images obtained at 1-day intervals. Appropriate X-ray images were regularly obtained at roughly 6-hr intervals through most of the Skylab mission and in some cases, which we discuss here, the observations were made at least once per orbit (≈ 90 min) for sequences of 3 to 7 consecutive orbits. We use these images to study coronal hole boundary changes on this substantially shorter time scale.

Analysis

The X-ray spectrographic telescope built by American Science and Engineering, Inc. flew on the Skylab spacecraft in 1973 and 1974. During the 8-month operational lifetime of the mission soft X-ray images of the sun were recorded on film with a spatial resolution of ≈ 2 arc sec. Six different broad-band filters and

a large dynamic range of exposure times were used to image various solar features and provide effective temperature diagnostics. The instrument has been described in detail by Vaiana et al. (1977), and an atlas of daily full-sun images of the X-ray corona was published by Zombeck et al. (1978).

The optimum images for studying the faint features of coronal holes are those obtained with the largest X-ray fluence. These are the 256 s exposures taken through the thinnest filter (filter 3) with passbands of 2-32 and 44-54 Å. Usable images in this mode were obtained from 1973 May 28 to November 21 (Nolte et al., 1976). We examined a catalog of all such sun-centered images obtained during 5-day periods centered on the CMPs of low-latitude coronal holes determined by Nolte et al. (1976) to look for images in three or more consecutive orbits. We restricted the images to those with coronal holes near CMP and limited the regions of interest to latitudes of $\pm 40^\circ$ to minimize the projection effects of optically thin structures at hole boundaries (Nolte et al., 1976). Since we wanted to study hole boundary changes, we sought large area holes with extensive boundaries. For that reason we eliminated the sequences of images of coronal holes 2 (on May 29 and August 18) and 3 (on August 12 and 13) because of their small areas (Nolte et al., 1976) and concentrated on Coronal Hole 1 (hereafter CH 1, following the designation used by Timothy et al. (1975) for the first coronal hole observed during the Skylab mission). The only images satisfying our requirements were obtained on 3 consecutive orbits on June 2, 7 orbits on August 19, 4 orbits on August 20, and 4 orbits on August 21.

Full-disk X-ray images of CH 1 at each CMP have been published by several authors (i.e., Figure 9 of Timothy et al. (1975); Figure 1 of Nolte et al. (1978c); and Figure 1 of Maxson and Vaiana (1977)) and will not be repeated here. It was the largest of the Skylab coronal holes, extending from the north pole to about S 20° with a width of order 15° at the equator. The extensive boundaries of the hole allow us a good opportunity to study the details of the boundary changes.

The changes of the hole boundaries were examined by a visual comparison of second-generation transparencies with a disk diameter of 10.8 cm. Since the positions of the boundaries and the changes in those positions over several consecutive orbits involves a subjective determination, we first listed all suspected boundary changes in all sets of images and then repeated the effort to get only the clearest examples. We eliminated cases where the area changes were so small as to be questionable or where the brightness change of a boundary feature was not sufficient to cause one to redraw the boundary. Although they claimed that coronal hole boundaries are sharp, Maxson and Vaiana (1977) presented cross sections of photographic density through the filter 3, 256 s images that clearly display the low spatial gradients of brightness at the boundary that render the boundary determination uncertain by perhaps 10-30 arc sec. Our boundary changes, characterized as one-dimensional features, ranged from ≈ 10 arc sec ($\approx 7 \times 10^3$ km) to ≈ 1 arc min (4.3×10^4 km). Our lower limit is slightly less than that ($\approx 1.2 \times 10^4$ km).

of Nolte et al. (1978a) who examined hole boundary shifts on a time scale of 1 day.

In the examination of the boundary changes it was immediately apparent that bright points played an important role. This can be seen in Figure 1, which shows the sequences of filter 3, 256 s images of CH 1 during the times of 7 consecutive orbits on August 19. In the figure black arrows point to the bright points associated with coronal hole expansions and white arrows point to the bright points associated with coronal hole shrinkages. One case of a hole shrinkage with no bright point association is shown with the lower white arrow at 0651 UT in Figure 1. In the images of August 20 and 21 there were two cases of coronal hole expansions without any observed associated bright point. In the images of all four dates we found 32 boundary changes of which 29 could clearly be associated with bright points.

The most common kind of boundary change is simply the appearance of a new bright point or the disappearance of a pre-existing bright point at the coronal hole boundary in such a way as to cause an apparent shift in the boundary by about the dimension of the bright point itself. Most of the boundary changes of Figure 1 are of this type. In some cases an X-ray region somewhat more extensive than just the bright point itself will brighten or dim. Two examples in Figure 1 are shown by the lower white arrow at 0226 UT, in which a relatively large X-ray structure in the hole attaches itself to the boundary, and by the black arrow at the eastern boundary at 0415 UT, where a large bright region surrounding the bright point slowly fades after the transient appearance of the bright point.

A summary of the time and size scales of the three kinds of boundary changes is given in Table 1, where we have averaged the measured sizes and the number of orbits over which the brightening or dimming of the X-ray structure was observed. Since the time resolution is ≈ 90 min, the actual time scales could be significantly less than the observed values, and we have given them as upper limits. To compare these boundary changes with those expected from supergranulation motions, we can use the time and size scales to calculate a characteristic speed for the boundary changes of $\geq 6 \times 10^3$ km hr⁻¹ for all categories of changes. Assuming a supergranulation cell size of 3.2×10^4 km and cell lifetime of 20 hr, we see that the speeds of the boundary changes exceed the supergranulation speed of 1.6×10^3 km hr⁻¹ by at least a factor of 4. These boundary changes are therefore not due to supergranulation motion.

The dimensions of the 32 observed boundary changes ranged from 7×10^3 km to 4.5×10^4 km with an average of 1.7×10^4 km; only one event exceeded 3.2×10^4 km. We therefore find no evidence for large scale boundary shifts of a size exceeding three times the supergranulation cell size ($\approx 9 \times 10^4$ km) discussed by Nolte et al. (1978a).

Most of the bright points associated with the boundary changes are much fainter than those used by Golub et al. (1974) for bright point statistics studies. Those authors used bright points visible on 4 s exposures, while we have used 256 s exposures. Comparing bright point counts in coronal holes on 4 s

and 256 s images, Golub et al. found about 100 times more bright points visible on the longer exposures. They also found a correlation between the maximum areas and the lifetimes of bright points. The bright points we have observed are generally small in area ($< 20 \times 10^7 \text{ km}^2$) and short lived (1-5 hrs), consistent with this correlation.

The tendency of CH 1 to rotate quasi-rigidly rather than to participate in the solar differential rotation was discussed by Timothy et al. (1975). To see whether the 32 boundary changes we found in the sequences of images contributed to that quasi-rigid rotation, we establish two categories of boundary changes. X-ray brightenings on the western boundary and dimmings on the eastern boundary of the hole result in an eastward shift of the hole boundary. Conversely, X-ray brightenings on the eastern boundary and dimmings on the western boundary shift the hole boundaries westward. We used Stoneyhurst disks to measure the latitude of each boundary change and then compared the eastward shifts with the westward shifts as a function of latitude. The summed results for all four dates are shown in Table 2. Coronal holes will be sheared by differential rotation as the low-latitude regions are shifted westward relative to the high-latitude regions. We see that within the limited statistics of Table 2 the observed shifts oppose the differential rotation by being predominately eastward at low ($\leq 20^\circ$) latitudes and westward at high ($> 20^\circ$) latitudes. This result may perhaps have been anticipated from our previous knowledge of the quasi-rigid rotation (Timothy et al., 1975), but it provides supporting evidence that the boundary changes associated with bright points are the changes important to the development of the coronal hole.

Discussion

Recent work on modeling coronal fields by the Naval Research Lab group (Nash et al., 1988) has provided an explanation for the rigid rotation of coronal holes near solar minimum. Using a potential field model with differential rotation, diffusion and meridional flow, they found that the outer coronal field rotates more rigidly than the underlying photospheric field because it depends on only the lowest-order harmonic components. The motion of the hole boundary is uncoupled from that of the underlying photospheric flux elements by continual reconnection of magnetic field lines. The details of the reconnection process are not specified. One possibility is that this reconnection occurs in the high corona. The time scale of the boundary changes ($\approx 1-5$ hrs) is consistent with this, but no bright point involvement would be expected.

The appearance of X-ray bright points in boundary changes suggests that we examine the weak photospheric fields for the source of the reconnection process. The structure of the magnetic fields at hole boundaries is characteristic of the quiet sun fields consisting of network clusters at supergranular cell vertices and of weaker intranetwork fields (Zwaan, 1987). The latter weak ($< 50 \text{ G}$) fields consist of mixed polarities and do not extend into the outer corona. We suggest that reconnection

occurs between the small-scale structure and the larger scale magnetic field as shown schematically in Figure 2. The X-ray bright points associated with the hole boundary changes may correspond to the small loop in A or C of the figure or to the reconnection region in B. The separatrix is drawn between the two closed field regions in C because it separated the small scale structure from the large scale structure and because the bright point will be faint either before the sequence C,B,A or after the sequence A,B,C. The size and time scales of the proposed reconnection scenario are those given in Table 1. A somewhat similar schematic was proposed by Marsh (1978) to explain the relationship between bright point flares and supergranulation network flux elements. He observed several cases of an H α brightening at the network element followed by a fibril system linking the network element with one of the poles of the bipolar region.

Nolte et al. (1978c) found a statistical relationship between the bright point density in coronal holes and the rate of shrinkage of the hole area. They suggested that this was due to two reasons. First, the hole was being filled in by X-ray-emitting closed-field remnants of the bright points. A problem with this idea is that we have no evidence that the bright points grow to the observed sizes of large-scale structures. The brightest bright points have lifetimes of less than a day (Golub et al., 1974). The second reason proposed by Nolte et al. (1978c) was that the bright points enhanced the rate of reconnection of open field lines at the hole boundaries. However, if a bright point reconnects with an open field line, one end of the bright point bipole must also be open after the reconnection process. Thus the proposed reconnection scenario will not result in a net closing of large-scale open field lines. In contrast, in our Figure 2 we see that the bright point in C interacts with adjacent closed field line flux to produce a shrinking of the hole area in the C,B,A sequence by motions of previously closed field lines. A further observational problem with the Nolte et al. idea is that a more detailed examination of the bright point densities in coronal holes by Davis (1985) showed no association between bright point density and the rates of hole growth or decay.

At the time of their discovery it was obvious that bright points were bipolar magnetic structures (Golub et al., 1974). They were interpreted as regions of emerging flux by Golub et al. (1974) and others. This view was challenged by Harvey (1985), who used He I 10830 Å dark points as a proxy for X-ray bright points and found that about two-thirds of the dark points were associated with chance encounters of features of opposite magnetic polarity. In a recent study Webb and Moses (1988) compared bright points observed in rocket solar X-ray images with bipoles observed in simultaneous videomagnetograms. The great majority of bipoles were not associated with X-ray bright points, but 11 of 16 observed X-ray bright points were associated with cancelling bipoles and only one with an emerging bipole. Webb and Moses concluded that their results were consistent with the Harvey (1985) interpretation that most bright points are

associated with encounters of opposite polarity features. Our observations suggest that the bright points form due to coronal heating at some time during the reconnection process. X-ray bright points are known to flare on a time scale of minutes (Golub et al., 1974), but it is not clear how the flare event or the formation and disappearance of the bright point are related to the reconnection scenario of Figure 2.

Acknowledgements. We thank D. Webb, E. Hildner, R. Moore, A. Nash, and N. Sheeley, Jr. for helpful comments. This research was supported at Emmanuel College by AFGL contract F19628-87-K-0033 and at AS&E by NASA contract NAS5-25496.

References

- Davis, J.M., Small-scale flux emergence and the evolution of equatorial coronal holes, Solar Phys., 95, 73-82, 1985.
- Golub, L., A.S. Krieger, J.K. Silk, A.F. Timothy, and G.S. Vaiana, Solar X-ray bright points, Ap.J., 189, L93-L97, 1974.
- Harvey, K.L., The relationship between coronal bright points as seen in He I 10830 and the evolution of the photospheric network magnetic fields, Aust. J. Phys., 38, 875-883, 1985.
- Krieger, A.S., Temporal behavior of coronal holes, in Coronal Holes and High Speed Wind Streams, edited by J.B. Zirker, Colorado Associated University Press, Boulder, 71-102, 1977.
- Marsh, K.A., Ephemeral region flares and the diffusion of the network, Solar Phys., 59, 105- 113, 1978.
- Maxson, C.W., and G.S. Vaiana, Determination of plasma parameters from soft X-ray images for coronal holes (open magnetic field configurations) and coronal large-scale structures (extended closed-field configurations), Ap.J., 215, 919-941, 1977.
- Nash, A.G., N.R. Sheeley, Jr., and Y.-M. Wang, Mechanisms for the rigid rotation of coronal holes, Solar Phys., 117, 359-389, 1988.
- Nolte, J.T., A.S. Krieger, A.F. Timothy, G.S. Vaiana, and M.V. Zombeck, An atlas of coronal hole boundary positions May 28 to November 21, 1973, Solar Phys., 46, 291-301, 1976.
- Nolte, J.T., A.S. Krieger, and C.V. Solodyna, Short term evolution of coronal hole boundaries, Solar Phys., 57, 129-139, 1978a.
- Nolte, J.T., M. Gerassimenko, A.S. Krieger, and C.V. Solodyna, Coronal hole evolution by sudden large scale changes, - SolarPhys., 56, 153-159, 1978b.
- Nolte, J.T., J.M. Davis, M. Gerassimenko, A.S. Krieger, C.V. Solodyna, and L. Golub, The relationship between solar activity and coronal hole evolution, Solar Phys., 60, 143-153, 1978c.
- Timothy, A.F., A.S. Krieger, and G.S. Vaiana, The structure and evolution of coronal holes, Solar Phys., 42, 135-156, 1975.
- Vaiana, G.S., L. van Speybroeck, M.V. Zombeck, A.S. Krieger, J.K. Silk, and A. Timothy, The S-054 X-ray telescope experiment on Skylab, Space Sci. Instr., 3, 19-76, 1977.
- Webb, D.F., and J.D. Moses, The correspondence between small-scale coronal structures and the evolving solar magnetic field, Advances Space Res., in press, 1988.
- Zombeck, M.V., G.S. Vaiana, R. Haggerty, A.S. Krieger, J.K. Silk, and A. Timothy, An atlas of soft X-ray images of the solar corona from Skylab, Ap.J. Supple., 38, 69-85, 1978.
- Zwaan, C., Elements and patterns in the solar magnetic field, - Ann.Rev.Astron.Astrophys., 25, 83-111, 1987.

TABLE 1. Time and Size Scales of Boundary Changes

<u>Boundary Change</u>	<u>Dimming</u>	<u>Brightening</u>
Bright Point Only	11 cases 1.3×10^4 km ≤ 2.3 hr	9 cases 1.4×10^4 km ≤ 1.8 hr
Bright Point and Extended Structure	6 cases 2.2×10^4 km ≤ 3.0 hr	3 cases 2.3×10^4 km ≤ 4.0 hr
Extended Structure Without Bright Point	2 cases 2.3×10^4 km ≤ 3.0 hr	1 case 2.0×10^4 km ≤ 3.0 hr

TABLE 2. Observed Boundary Shifts of CH 1

<u>Shifts</u>	<u>Latitude</u>			
	<u>01°-10°</u>	<u>11°-20°</u>	<u>21°-30°</u>	<u>31°-40°</u>
Eastward	4	9	2	1
Westward	3	4	6	3

Fig. 1. Skylab X-ray images of CH 1 during seven consecutive orbits on 1973 August 19. The five bright points which were associated with expansions of the hole area are shown by black arrows; the six bright points associated with hole shrinkage by white arrows. One case of a hole shrinkage with no obvious bright point association is shown by the lower white arrow at 0651 UT.

Fig. 2. Schematic for reconnection of magnetic fields at coronal hole boundaries. Dotted regions are closed fields; the wavy line is the separatrix between open and closed fields. Reconnection occurs in B in the shaded region. The sequence A,B,C corresponds to an expansion of the hole area; C,B,A corresponds to a shrinking of the hole area.



0032 UT



0226 UT



0415 UT



0512 UT



0651 UT

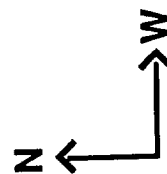


0818 UT

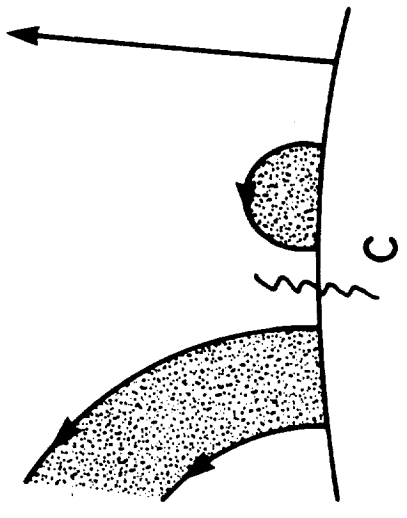
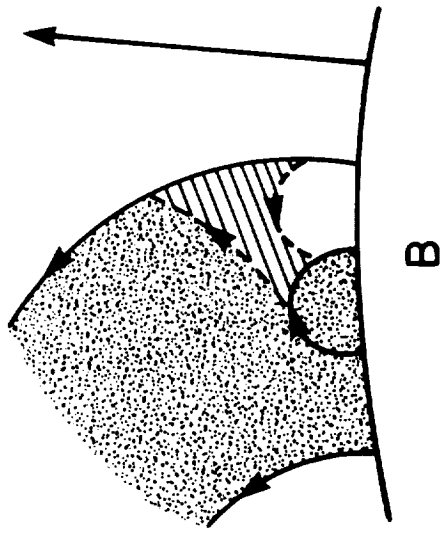
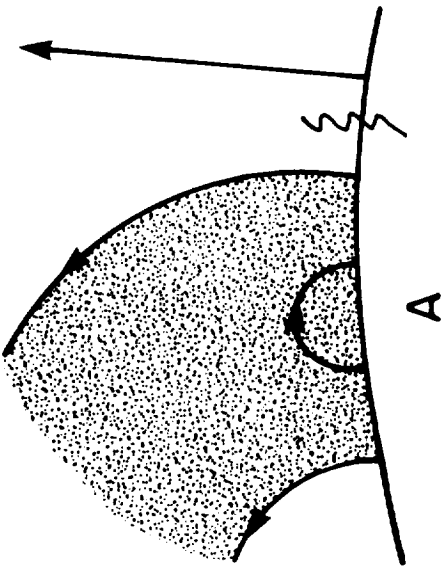


0952 UT

15 ARC MIN



19 AUGUST 1973



4.21 X-Ray Bright Points and He I 10830 Dark Points

L. Golub

Smithsonian Astrophysical Observatory
Cambridge, Massachusetts 02138

K.L. Harvey

Solar physics Research Corporation
Tucson, Arizona

M. Herant

Harvard University
Cambridge, Massachusetts 02138

and

D.F. Webb

Emmanuel College, Boston, Massachusetts
and
American Science and Engineering, Inc.
Cambridge, Massachusetts 02139

ORIGINAL PAGE IS
OF POOR QUALITY

1
2
3
4
5
6
7
8
9
10
11
12
13
14
15
16
17
18
19
20
21
22
23
24
25
26
27
28
29
30
31
32
33
34
35
36
37
38
39
40
41
42
43
44
45
46
47
48
49
50
51
52
53
54
55
56
57
58
59
60
61
62
63
64
65
66
67
68
69
70
71
72
73
74
75
76
77
78
79
80
81
82
83
84
85
86
87
88
89
90
91
92
93
94
95
96
97
98
99
100
101
102
103
104
105
106
107
108
109
110
111
112
113
114
115
116
117
118
119
120
121
122
123
124
125
126
127
128
129
130
131
132
133
134
135
136
137
138
139
140
141
142
143
144
145
146
147
148
149
150
151
152
153
154
155
156
157
158
159
160
161
162
163
164
165
166
167
168
169
170
171
172
173
174
175
176
177
178
179
180
181
182
183
184
185
186
187
188
189
190
191
192
193
194
195
196
197
198
199
200
201
202
203
204
205
206
207
208
209
210
211
212
213
214
215
216
217
218
219
220
221
222
223
224
225
226
227
228
229
230
231
232
233
234
235
236
237
238
239
240
241
242
243
244
245
246
247
248
249
250
251
252
253
254
255
256
257
258
259
260
261
262
263
264
265
266
267
268
269
270
271
272
273
274
275
276
277
278
279
280
281
282
283
284
285
286
287
288
289
290
291
292
293
294
295
296
297
298
299
300
301
302
303
304
305
306
307
308
309
310
311
312
313
314
315
316
317
318
319
320
321
322
323
324
325
326
327
328
329
330
331
332
333
334
335
336
337
338
339
340
341
342
343
344
345
346
347
348
349
350
351
352
353
354
355
356
357
358
359
360
361
362
363
364
365
366
367
368
369
370
371
372
373
374
375
376
377
378
379
380
381
382
383
384
385
386
387
388
389
390
391
392
393
394
395
396
397
398
399
400
401
402
403
404
405
406
407
408
409
410
411
412
413
414
415
416
417
418
419
420
421
422
423
424
425
426
427
428
429
430
431
432
433
434
435
436
437
438
439
440
441
442
443
444
445
446
447
448
449
450
451
452
453
454
455
456
457
458
459
460
461
462
463
464
465
466
467
468
469
470
471
472
473
474
475
476
477
478
479
480
481
482
483
484
485
486
487
488
489
490
491
492
493
494
495
496
497
498
499
500
501
502
503
504
505
506
507
508
509
510
511
512
513
514
515
516
517
518
519
520
521
522
523
524
525
526
527
528
529
530
531
532
533
534
535
536
537
538
539
540
541
542
543
544
545
546
547
548
549
550
551
552
553
554
555
556
557
558
559
560
561
562
563
564
565
566
567
568
569
570
571
572
573
574
575
576
577
578
579
580
581
582
583
584
585
586
587
588
589
590
591
592
593
594
595
596
597
598
599
600
601
602
603
604
605
606
607
608
609
610
611
612
613
614
615
616
617
618
619
620
621
622
623
624
625
626
627
628
629
630
631
632
633
634
635
636
637
638
639
640
641
642
643
644
645
646
647
648
649
650
651
652
653
654
655
656
657
658
659
660
661
662
663
664
665
666
667
668
669
670
671
672
673
674
675
676
677
678
679
680
681
682
683
684
685
686
687
688
689
690
691
692
693
694
695
696
697
698
699
700
701
702
703
704
705
706
707
708
709
710
711
712
713
714
715
716
717
718
719
720
721
722
723
724
725
726
727
728
729
730
731
732
733
734
735
736
737
738
739
740
741
742
743
744
745
746
747
748
749
750
751
752
753
754
755
756
757
758
759
760
761
762
763
764
765
766
767
768
769
770
771
772
773
774
775
776
777
778
779
780
781
782
783
784
785
786
787
788
789
790
791
792
793
794
795
796
797
798
799
800
801
802
803
804
805
806
807
808
809
810
811
812
813
814
815
816
817
818
819
820
821
822
823
824
825
826
827
828
829
830
831
832
833
834
835
836
837
838
839
840
84